

Axial and Radial Hydraulic Resistance to Roots of Maize (*Zea mays* L.)¹

Jürgen Frensch* and Ernst Steudle

Lehrstuhl für Pflanzenökologie, Universität Bayreuth, Universitätsstr. 30, D-8580
Bayreuth, Federal Republic of Germany

ABSTRACT

A root pressure probe was employed to measure hydraulic properties of primary roots of maize (*Zea mays* L.). The hydraulic conductivity (L_p) of intact root segments was determined by applying gradients of hydrostatic and osmotic pressure across the root cylinder. In hydrostatic experiments, L_p was constant along the segment except for an apical zone of approximately 20 millimeters in length which was hydraulically isolated due to a high axial resistance. In osmotic experiments, L_p decreased toward the base of the roots. L_p (osmotic) was significantly smaller than L_p (hydrostatic). At various distances from the root tip, the axial hydraulic resistance per unit root length (R_x) was measured either by perfusing excised root segments or was estimated according to Poiseuille's law from cross-sections. The calculated R_x was smaller than the measured R_x by a factor of 2 to 5. Axial resistance varied with the distance from the apex due to the differentiation of early metaxylem vessels. Except for the apical 20 millimeters, radial water movement was limiting water uptake into the root. This is important for the evaluation of L_p of roots from root pressure relaxations. Stationary water uptake into the roots was modeled using measured values of axial and radial hydraulic resistances in order to work out profiles of axial water flow and xylem water potentials.

radial (R_R)² and an axial (R_x) component and their relative importance for the root to collect and to transport water has been stressed (9, 11, 12, 18). However, reasonable quantitative data of R_x and R_R are rare, although they are a prerequisite for a proper modeling of water flows across roots. Previous studies on end segments of primary roots using the root pressure probe (20–23) suggested that, to some extent, R_x of the xylem may contribute to the overall resistance (20, 21). A contribution of R_x could be important because the radial hydraulic conductivity (L_{pr}) is commonly evaluated neglecting R_x . This is true for usual exudation experiments, pressurized exudation (3), and stop-flow techniques (8, 10, 15) as well as for the root pressure probe (19–23). Therefore, the radial versus the axial hydraulic resistances of excised primary roots of maize seedlings have been measured in this paper in order to work out their relative importance for limiting the water uptake by roots. In addition, the dependence of the hydraulic conductivity on the nature of the driving force has been investigated in relation to the variability of the hydraulic conductivity (L_{pr}) along the root. The results have been used to model hydraulic properties of roots and to calculate profiles of the rates of axial water flow and xylem water potential according to a mathematical treatment originally introduced by Landsberg and Fowkes (9).

MATERIALS AND METHODS

Plant Material

Experiments were carried out on primary roots of 3 to 16 d old plants of *Zea mays* L. cv 'Tanker' grown in hydroculture. The methods employed in germination and in growing the seedlings have been described in detail elsewhere (21, 23).

² Abbreviations: R_R , radial hydraulic resistance (per unit of effective surface area); R_x , axial hydraulic resistance (per unit length); a , radius of the root; A_r , geometric surface area of the root; A_r^{eff} , effective surface area of the root; J_{vr} , radial volume flow across the root; k_{wr} , rate constant of water exchange between root xylem and medium; l , root length; L , total hydraulic conductance; L_x , axial hydraulic conductance; L_{pr} , radial hydraulic conductivity (per unit of effective root surface area); L_{pr}^{app} , apparent radial hydraulic conductivity (per unit of geometric root surface area); P_r , root pressure; q_R , radial water flow across the root; q_T , total water flow across the root; q_x , axial water flow across the root at a certain distance from the root tip; z , r , radius of a conductive xylem vessel; V_s , volume of the measuring system; z , position along the root; α , inverse of the half-length of a drop of Ψ_x ; Ψ_s , water potential of the nutrient solution; Ψ_x , water potential of the xylem.

The uptake of water from the soil and its transport to the shoot is an essential function of the root system. The movement of water across the root is driven by water potential differences and limited by hydraulic resistances. It is commonly thought that in the transpiring plant, water uptake is purely passive and mainly follows a hydrostatic pressure gradient between the root surface and xylem. Since there is an osmotic barrier in the root, a concentration difference of solutes between the xylem and the surrounding soil solution will also act as a driving force for water movement. Thus, hydrostatic and osmotic pressure components do occur in the intact root, and they may contribute differently to the overall water flow under different conditions (19).

The overall hydraulic resistance has been separated into a

¹ Supported by the Deutsche Forschungsgemeinschaft, Sonderforschungsbereich 137.

The nutrient solution contained the following major components (in mM) K^+ (1.5), NH_4^+ (2.0), Ca^{2+} (0.75), Mg^{2+} (1.0), NO_3^- (4.0), SO_4^{2-} (0.75), and PO_4^{3-} (0.75), along with a solution containing micronutrients and Fe-EDTA (0.04 mM; pH = 6.0).

Measurement of Root Hydraulic Conductivity

Excised segments of roots free of visible laterals (length, 18–140 mm; diameter, 1.0–1.4 mm) were sealed to a root pressure probe with the aid of silicone rubber seals (Fig. 1). Within 30 min the root pressure increased to a stationary value which slightly decreased at the end of a 12 h period of experiments. However, this decline was much slower than the time constants of the pressure changes (relaxations) induced by the experimental procedures to measure the hydraulic conductivity. Effects of aging or of diurnal changes of water relations parameters during the measurements could not be detected. The hydraulic conductivity of a root segment (per m^2 of root surface area; see below) was determined by applying hydrostatic and osmotic pressure gradients across the root to induce radial water flows. In hydrostatic experiments, P_r was changed by pushing water into the cut end of the root with the aid of the metal rod or by withdrawing it. In osmotic experiments, the bathing medium was changed instantaneously to solutions containing test solutes in certain concentrations. Both types of experiments resulted in root pressure relaxations caused by a radial water movement into or out of the root with certain rate constants, k_{wr} , which depended on the radial hydraulic conductivity, Lp_r . The Lp_r referring to the geometrical surface area of the root (A_r) was called 'apparent' hydraulic conductivity (Lp_r^{app}) because only part of the entire surface area was conducting water. The hydraulic conductivity referring to this effective area (A_r^{eff}) was called Lp_r or corrected Lp_r . The theory for calculating Lp_r from

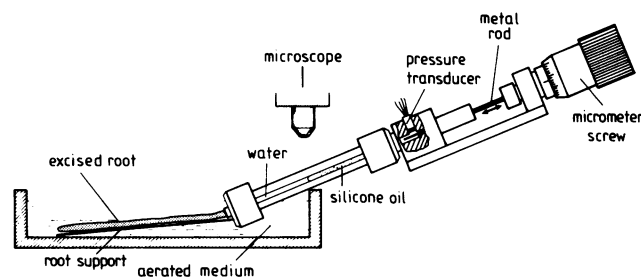


Figure 1. Root pressure probe for measuring water relations parameters of excised roots. The root was tightly connected to the probe by a silicone seal so that root pressures could be built up in the system which could be recorded continuously with the aid of a pressure transducer. A meniscus between silicone oil and water within a measuring capillary served as a reference during the measurements. Water flow across the root could be induced either by changing the hydrostatic pressure in the probe by moving a metal rod with the aid of a micrometer screw or by exchanging the root medium by a medium containing a test solute of known osmotic pressure. Measurements were carried out on (a) closed (intact) segments, on (b) open (cut) segments, and on (c) root segments of short length (18 mm) within the silicone seal (see insets of Figs. 3–5) in order to determine the hydraulic conductivity for the radial movement of water (Lp_r) and the axial hydraulic resistance (R_x).

pressure relaxations has been given in detail in previous papers (20–23). k_{wr} is related to Lp_r^{app} or Lp_r by

$$k_{wr} = Lp_r^{app} \cdot A_r \frac{\Delta P_r}{\Delta V_s} = Lp_r \cdot A_r^{eff} \frac{\Delta P_r}{\Delta V_s} = \frac{1}{R_R} \cdot A_r^{eff} \frac{\Delta P_r}{\Delta V_s} \quad (1)$$

$\Delta P_r / \Delta V_s$ = elasticity of the measuring system in $MPa \cdot m^{-3}$ (= inverse of the water capacitance); R_R = radial hydraulic resistance per unit surface area ($MPa \cdot s \cdot m^{-1}$). Strictly, Equation 1 is only valid at a negligible axial resistance. This may not be true, since the xylem develops in the apical zone of the root, where it should exhibit a considerable resistance due to cross-walls and membranes of living cells. In this region, Lp_r^{app} will be small. The effect of xylem development can be taken into account in the calculation of Lp_r by measuring Lp_r^{app} as a function of root length.

Measurement of Axial Resistance

Axial hydraulic resistances (R_x = hydraulic resistance of the root per unit length of root) were evaluated from two different types of experiments. In the first one, R_x was determined by cutting the root successively with a razor blade at certain distances from the tip. As soon as conducting xylem vessels were hit, P_r dropped to a lower pressure. When a new steady P_r was reached, a hydrostatic experiment was per-

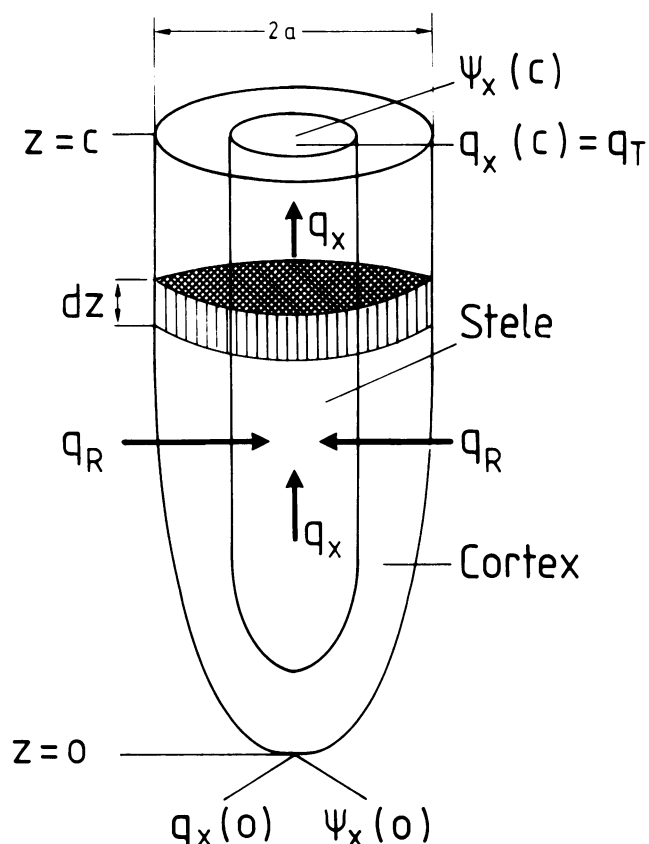


Figure 2. Illustration of the radial (q_R) and axial (q_x) components of water flow in a root which vary due to the collection of water by the root with the distance from the root apex, z . For further explanations, see text.

formed. Since the hydraulic capacitance of the system remained constant during the experiment (21), a change of the total hydraulic conductance ($L = L_{pr} \cdot A_r^{eff} + L_x$) can be directly measured from a change in k_{wr} . It is valid that

$$k_{wr} = L \cdot \frac{\Delta P_r}{\Delta V_s}. \quad (2)$$

During the cutting experiments, conducting surface (A_r^{eff}) was removed whereas L_x increased, *i.e.* the axial and radial conductances changed simultaneously but in opposite directions. The effects can be separated by measuring L_{pr}^{app} as a function of root length from relaxations performed on intact root segments having a closed tip, and the axial component from cut segments (see below).

According to Poiseuille's law, the hydraulic conductance of the root xylem would be

$$L_x = \frac{\pi \cdot n \cdot r^4}{8 \cdot \eta \cdot \ell}, \quad (3)$$

provided that the xylem vessels can be treated as circular tubes of constant diameter. η = viscosity of water ($1 \cdot 10^{-9}$ MPa·s at 20°C); n = number of conducting xylem elements; r = radius of conducting elements; ℓ = length of conducting elements. The hydraulic resistance per unit length, R_x , would be

$$R_x = \frac{1}{L_x \cdot \ell}. \quad (4)$$

R_x can be obtained from plots of L_x as a function of $1/\ell$ in open-ended segments provided that the radial component of water flow can be neglected compared with the axial.

In the second type of experiments, roots of different length were mounted on the probe, and were cut right at the seal. Hydrostatic pressure relaxations were performed using only the remaining piece of the root within the seal (18 mm). Under these conditions, radial water flow was negligible, and R_x could be determined in relation to the original position of the segment in the intact root. The resolution of the pressure probe was tested to be sufficiently high to detect much smaller R_x than those determined in this study.

Calculation of Axial Hydraulic Resistance (R_x)

Xylem anatomical studies were carried out on free-hand cross-sections made at distances of 10, 20, 40, 80, and 140 mm from the root tip. The sections were stained with 'toluidine blue O' to identify mature xylem. Mean diameters were obtained from photographs of the sections and were used to estimate R_x according to Equations 3 and 4 (Table I).

Calculation of Steady Water Flow and of Xylem Water Potential Profiles Along the Root

Provided that R_R and R_x of a root are known, profiles of xylem water potential (Ψ_x) and of the flow rate in the xylem (q_x) can be evaluated in hydrostatic experiments for stationary conditions according to Landsberg and Fowkes (9). For an unbranched root segment (Fig. 2), the radial flow of water (q_R) in $\text{m}^3 \cdot \text{m}^{-2} \cdot \text{s}^{-1}$ following a potential gradient between the xylem and its surroundings (soil, nutrient solution) is given by

$$q_R(z) = \frac{\Psi_s(z) - \Psi_x(z)}{R_R(z)}, \quad (5)$$

where Ψ_s = water potential of the surroundings. In principle, Ψ_s , Ψ_x , R_R , and q_x may vary along the root, *i.e.* they should be functions of the distance from the root tip (z). The axial flow component, q_x (in $\text{m}^3 \cdot \text{s}^{-1}$), will be related to the axial resistance and to the gradient of the water potential in the xylem by

$$q_x(z) = - \frac{1}{R_x(z)} \cdot \frac{d\Psi_x}{dz}. \quad (6)$$

Conservation of matter requires that the change in $q_x(z)$ over a distance of dz would be (Fig. 2):

$$\frac{dq_x}{dz} = 2 \cdot \pi \cdot a \cdot q_R(z), \quad (7)$$

where a is the radius of the root. Combining Equations 5 to 7 yields

$$\frac{d^2\Psi_x}{dz^2} = \alpha^2 \cdot (\Psi_x - \Psi_s) \quad (8)$$

with

$$\alpha^2 = 2 \cdot \pi \cdot a \cdot \frac{R_x}{R_R}. \quad (9)$$

The meaning of α is that of an inverse of a half-length of a drop of Ψ_x , *i.e.* with increasing values of α , gradients of xylem water potential are steeper. A solution of Equation 8 was provided by Landsberg and Fowkes (9). They assumed that R_R , R_x = constant, *i.e.* that the parameters did not change along the root axis. However, our results showed that R_x did vary so that from Equations 5 to 7 a different result was obtained, namely

$$\begin{aligned} \frac{d^2\Psi_x}{dz^2} = 2 \cdot \pi \cdot a \cdot \frac{R_x(z)}{R_R} \cdot (\Psi_x - \Psi_s) \\ + \frac{d\Psi_x}{dz} \cdot \frac{1}{R_x(z)} \cdot \frac{dR_x(z)}{dz}. \end{aligned} \quad (10)$$

This differential equation was numerically solved on a personal computer assuming a constant Ψ_s along the root to get $\Psi_x(z)$ and $q_x(z)$ at given $R_x(z)$ and $R_R(z)$ characteristics. With respect to the function of the root the total amount of water taken up ($q_T = q_x(c)$) is important. This will be given by (9)

$$q_T = \frac{1}{R_x(c)} \cdot \left(\frac{d\Psi_x}{dz} \right)_c. \quad (11)$$

RESULTS

In hydrostatic experiments, the apparent hydraulic conductivity per m^2 of root surface area (L_{pr}^{app}) steadily increased with root length (Fig. 3A). The relationship between L_{pr}^{app} and ℓ which was fitted by a polynomial of third order indicated very low L_{pr}^{app} values at $\ell < 15$ mm from the root tip. This finding corresponded with earlier studies which showed that cutting off 10 to 20 mm of the root tip had little effect on the

Table 1. Geometrical Data of Mature Xylem Elements of the Root Segments used in This Study

Mean values of the number of mature xylem elements and total area of mature xylem were obtained from 5 individual roots (5–7 d old seedlings) which were cross-sectioned at several distances from the root apex. Diameters of vessels of mature protoxylem and of early metaxylem were constant (4 ± 1 and $22 \pm 3 \mu\text{m}$, respectively). Note that elements of late metaxylem were not mature within the observed range and, therefore, are not included in the table. All data are given \pm SD; number of measured sections, $n = 3$ –5.

Measurement	Distance from the Root Apex (m):				
	0.01	0.02	0.04	0.08	0.14
Number of elements of mature protoxylem	20 ± 2	21 ± 4	21 ± 4	20 ± 2	20 ± 2
Number of elements of mature early metaxylem	0	2 ± 2	18 ± 4	17 ± 3	18 ± 2
Total area of mature xylem in % of cross-section area	0.05 ± 0.01	0.16 ± 0.18	1.1 ± 0.3	1.1 ± 0.3	1.2 ± 0.3

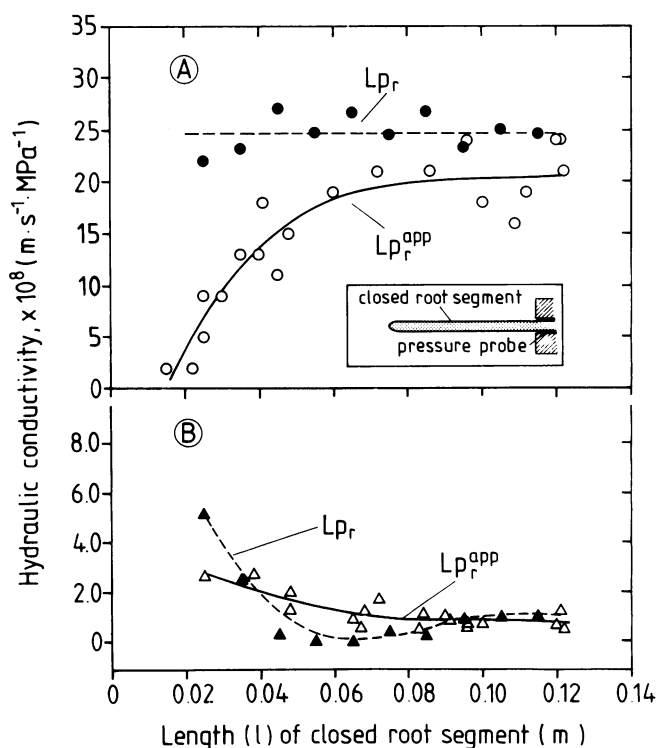


Figure 3. Dependence of the hydraulic conductivity of intact (closed) root segments of maize plants on the length of the segment as determined in hydrostatic (A) and osmotic (B) experiments. Values of the apparent hydraulic conductivity ($L_{p_r}^{app}$) refer to the geometric surface area, A_r , whereas L_{p_r} refers to the effective surface area (A_r^{eff}) which excludes the tip region (about 15 mm from the root apex). L_{p_r} (hydrostatic) was larger than L_{p_r} (osmotic) by an order of magnitude and was constant throughout the segment, while L_{p_r} (osmotic) decreased with increasing distance from the root apex.

apparent L_{p_r} (21). Therefore, it was assumed that the apical end was hydraulically isolated from the rest of the root, and the data were recalculated for root segment intervals of 10 mm length using the effective surface area, i.e. the geometric surface area minus the surface area of the root tip. The corrected values of L_{p_r} showed no dependence on root length (Fig. 3A). This indicated that L_{p_r} was fairly constant along

the conducting part of the root and that the curvilinear behavior of $L_{p_r}^{app}$ was due to an overestimation of the surface area. The absolute value of the corrected L_{p_r} was $25 \pm 2 \cdot 10^{-8} \text{ m} \cdot \text{s}^{-1} \cdot \text{MPa}^{-1}$ (mean \pm SD, $n = 10$ intervals). Osmotically induced flows revealed values of $L_{p_r}^{app}$ ranging from 0.5 to $2.7 \cdot 10^{-8} \text{ m} \cdot \text{s}^{-1} \cdot \text{MPa}^{-1}$ with an increase toward the apex (Fig. 3B). After correcting L_{p_r} to effective root surface areas it was found that, in contrast to the hydrostatic experiments, the relative changes of L_{p_r} with root length were even more pronounced. In accordance with previous results, the osmotic L_{p_r} was remarkably smaller than the hydrostatic L_{p_r} (21, 23).

Axial hydraulic conductances per unit root length (L_x) were evaluated from cutting experiments. Cutting resulted in an increase of L_x and in a decrease of radial conductance ($L_{p_r} \cdot A_r^{eff}$). However, from the measured values of the total conductance (L), L_x could be obtained by subtracting $L_{p_r} \cdot A_r^{eff}$ from L . It was found that L_x increased when roots became shorter (Fig. 4A). This effect could have been due to the progressive development of the xylem or simply due to the reduced root length according to Poiseuille's law (Eq. 3). To test whether xylem development occurred along the segments, L_x was plotted as a function of the reciprocal of the length of the attached root. For each individual root as well as for the mean of all roots ($n = 14$), a linear relationship was found in the range between 15 and 140 mm behind the root apex (Fig. 4B, individual data not shown). The mean of the slope was $L_x \cdot l = 52 \cdot 10^{-12} \text{ m}^4 \cdot \text{MPa}^{-1} \cdot \text{s}^{-1}$ which corresponded to an axial hydraulic resistance (per unit length) of $R_x = 19 \cdot 10^9 \text{ MPa} \cdot \text{s} \cdot \text{m}^{-4}$. The linear behavior of the slope in Figure 4B indicated a fairly good agreement with Equation 3 and, hence, it could be concluded that xylem development did not substantially influence R_x at distances between 15 and 140 mm for the apex. Usually it was valid that $L_{p_r} \cdot A_r^{eff} \ll L_x$ (compare absolute values of L_x in Figure 4B with those of $L_{p_r} \cdot A_r^{eff}$ in the inset of the same figure) and, therefore, changes of the total hydraulic conductance with root length were mainly due to changes of the absolute value of L_x .

Results similar to those found in cutting experiments were obtained from hydrostatic measurements performed on pieces of roots kept within the silicone seal (length: 18 mm). Pieces were obtained from end segments at different distances from the apex. With increasing distance (z), the axial resistance per

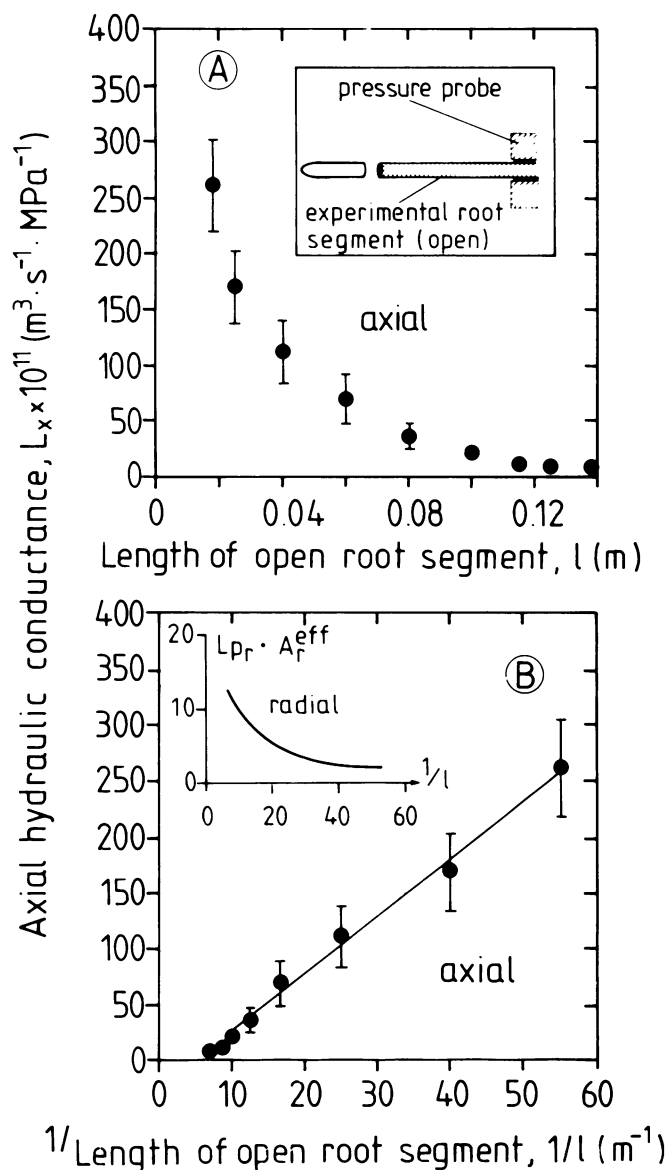


Figure 4. Axial hydraulic conductance, L_x , of cut root segments as a function of the remaining root length, l (A) or of the inverse, $1/l$ (B). Mean values are given \pm sd ($n = 14$ roots). Linear regression of the data between $z = 15$ and 140 mm yielded a slope of $52 \cdot 10^{-12} \text{ m}^4 \cdot \text{s}^{-1} \cdot \text{MPa}^{-1}$, which was equivalent to the hydraulic resistance of the xylem per unit root length, $R_x = 19 \cdot 10^9 \text{ MPa} \cdot \text{s} \cdot \text{m}^{-4}$. From the inset (B) it can be seen that changes induced by cutting were much smaller for radial conductance ($L_{pr} \cdot A_r^{\text{eff}}$) than for axial conductance, (L_x), i.e. that the total conductance $L = L_{pr} \cdot A_r^{\text{eff}} + L_x$, mainly changed due to changes of L_x .

unit length (R_x) decreased by two orders of magnitude within the apical 30 mm (Fig. 5; linear and logarithmic plot). This reflected a substantial increase of the contribution of conducting xylem elements between 0 and 30 mm from the apex. For segments beyond this position, R_x was fairly constant. For $80 \text{ mm} < z < 140 \text{ mm}$, a mean value of $R_x = 48 \pm 24 \cdot 10^9 \text{ MPa} \cdot \text{s} \cdot \text{m}^{-4}$ ($n = 18$ roots) was evaluated. In Figure 5, estimates of R_x for protoxylem and for protoxylem and early metaxylem using the results from cross-sections and

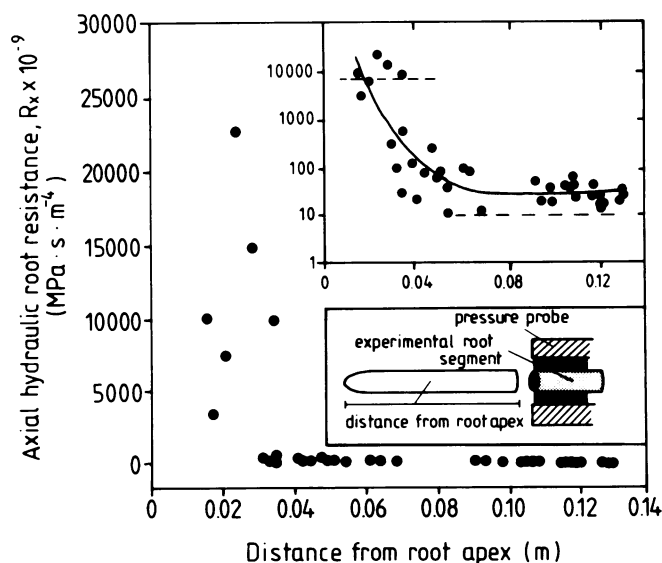


Figure 5. Axial hydraulic resistance, R_x , measured on root pieces of a length of 18 mm cut at different distances from the apex (z). R_x is plotted over the middle of the intervals and each data point represents an individual root (39 roots in total). Linear and log plots are given because of the large variation of R_x along the root axis. A polynomial of third order was used to fit the data points. This fit was used in the calculation of root profiles (see Eqs. 7–11 and Fig. 6). Dashed lines indicate estimated resistances according to Poiseuille's law obtained from cross-sections of roots assuming that protoxylem ($R_x = 7200 \cdot 10^9 \text{ MPa} \cdot \text{s} \cdot \text{m}^{-4}$) or early metaxylem ($R_x = 10 \cdot 10^9 \text{ MPa} \cdot \text{s} \cdot \text{m}^{-4}$) was conductive.

Poiseuille's law are indicated by dashed lines. They show that within the first 10 mm from the root apex only protoxylem should have been conductive. Between 10 and 40 mm, early metaxylem gradually matured. In the upper part of the root, the measured R_x was by a factor of 5 larger than the calculated (Fig. 5). Table II summarizes the results obtained from measurements (Figs. 3–5) and calculations (Table I). Despite differences in R_x , it was found that axial resistance was much smaller than radial.

The data points of R_x measured as a function of the distance from the apex were fitted by a polynomial of third order (Fig. 5). According to Equations 7 to 10, profiles of α ($\sim [R_x/R_R]^{1/2}$; Eq. 9), Ψ_x , and q_x , were calculated for steady state conditions using the measured, variable values of $R_x(z)$ and $R_R(z)$ (Fig. 6). For comparison, two constant values of R_x have also been employed in order to get profiles at a low ($\alpha = 4.5 \text{ m}^{-1}$) and a high ($\alpha = 45 \text{ m}^{-1}$) ratio of constant R_x/R_R . The calculations assumed that there were (a) a tension of -1 MPa (-10 bars) at the cut end of the segment (length, 120 mm; diameter, 1.3 mm), (b) a water potential in the medium of $\Psi_s = 0$, and (c) no osmotic pressure component in the xylem. For $z > 20$ mm, values of $R_x(z)$ were based on the fit given in Figure 5. For $z < 20$ mm a constant value of R_x was used according to the estimates for the protoxylem using Poiseuille's law ($R_x = 7 \cdot 10^{12} \text{ MPa} \cdot \text{s} \cdot \text{m}^{-4}$). Values of R_R were obtained from Figure 3A assuming a constant L_{pr} between 0 and 120 mm root length. No profiles have been calculated for R_R obtained from osmotic experiments (Fig. 3B) since the assumptions to de-

Table II. Calculated and Measured Hydraulic Resistances of Root Segments

Axial resistances per unit length (R_x) were calculated according to Equations 3 and 4 using the data of Table I. For comparison, also the measured radial ($1/[Lp_r \cdot A^{eff} \cdot l]$) and axial (R_x) resistances per unit root length in the range between 0.04 and 0.14 m from the root apex are shown which were obtained from Figures 3A, 4B, and 5. All data are given \pm SD.

Measurement	Distance from the Root Apex (m):				
	0.01	0.02	0.04	0.08	0.14
Calculated axial resistance	7600	87	9.7	10.2	9.7
$R_x \times 10^{-9}$ (MPa s m ⁻⁴)	± 3900	± 91	± 5.6	± 5.9	± 5.4
Measured radial resistance (Fig. 3)	—	—	$\leftarrow 830 \pm 60$ (n = 10) \rightarrow		
$1/[Lp_r \cdot A^{eff} \cdot l] \times 10^{-9}$ (MPa s m ⁻⁴)	—	—			
Measured axial resistance (Fig. 4)	—	—	$\leftarrow 19^* \pm 5$ (n = 14) \rightarrow		
$R_x \times 10^{-9}$ (MPa s m ⁻⁴)	—	—			
Measured axial resistance (Fig. 5)	—	—	$\leftarrow 48^* \pm 24$ (n = 18) \rightarrow		
$R_x \times 10^{-9}$ (MPa s m ⁻⁴)	—	—			

* Measured values significantly different from calculated at $P < 0.05$ (t test).

scribe osmotical induced water flow were different from those in the model of Landsberg and Fowkes (9).

In the calculation based on measured resistances, the variability of R_x/R_r along the root resulted in a steep gradient of Ψ_x in the apical 35 mm, whereas $\Psi_x(z)$ increased slowly in the rest of the segment. Radial and axial water flows were influenced by a change of Ψ_x (Eqs. 5 and 6). The axial water flow (q_x) increased monotonously between 25 and 120 mm from the root apex. The apical 20 mm did not contribute significantly to q_x . This result can be explained by the steep gradient of R_x in the tip region. The total flow of water across the root segment (q_T) following a hydrostatic pressure gradient of -1.0 MPa was $q_T = 8.6 \cdot 10^{-11} \text{ m}^3 \cdot \text{s}^{-1}$ ($=0.086 \mu\text{L} \cdot \text{s}^{-1}$). When the pressure gradient was varied in the model, a proportional change of the absolute value of $q_x(c)$ was found without affecting the shape of the profiles. Assuming that the vessels of the early metaxylem were conductive throughout the root ($\alpha = 4.5 \text{ m}^{-1}$) strongly reduced the gradient of Ψ_x and increased q_T ($q_T = 10.7 \cdot 10^{-11} \text{ m}^3 \cdot \text{s}^{-1} = 0.107 \mu\text{L} \cdot \text{s}^{-1}$). In the case of $\alpha = 45 \text{ m}^{-1}$, i.e. increasing R_x by a factor of 100 relative to R_r , Ψ_x changed rapidly in the basal parts of the root and water uptake was mainly restricted to these zones ($q_T = 2.2 \cdot 10^{-11} \text{ m}^3 \cdot \text{s}^{-1} = 0.022 \mu\text{L} \cdot \text{s}^{-1}$).

DISCUSSION

The results indicate that (a) the apical root zone (up to 15–20 mm from the tip) was ineffective in collecting water, (b) Lp_r was rather constant along the rest of the root segment in hydrostatic, but not in osmotic experiments, and (c) the axial resistance of the xylem (R_x) did not vary substantially between 40 and 140 mm from the apex. Measured values of R_x were smaller by a factor of 2 and 5 than those calculated according to Poiseuille's law. Except for the apical zone, the radial hydraulic resistance (R_r) was much more important in limiting water uptake than the axial hydraulic resistance (R_x).

The hydraulic conductivity of the roots was dependent on the nature of the pressure gradient applied. The difference between hydrostatic and osmotic conductivity has been ex-

plained in terms of a root model with different parallel pathways for radial water movement exhibiting different hydraulic conductivities (19–23). In hydrostatic experiments with maize, water flow appeared to be predominantly apoplastic, whereas in osmotic experiments there was a substantial cell-to-cell transport. Different species may exhibit a different pattern in radial pathways for water movement (19, 20). The constant Lp_r (hydrostatic) found in the present experiments may, thus, point to a rather constant apoplastic conductance in the root segments up to a root length of about 140 mm, although a decrease in the more basal parts (at $z > 140$ mm) cannot be excluded. Therefore, the finding does not necessarily contradict the usual picture of a maximum of water absorption in a zone just behind the elongating region. Differentiation occurred along the segments showing, for example, lateral root emergence at 60 mm from the apex (21). Secondary root initials could have provided an additional conductive area for radial water flow (14). In barley roots, the rate of water uptake measured under transpiring conditions (hydrostatic gradient) corresponded well with the developmental state of the endodermis when the water uptake across the laterals was prevented (17).

In contrast to the hydrostatic experiments, the osmotic experiments did show a decline in Lp_r (Fig. 3). Similar results for maize roots have recently been obtained by Jones *et al.* (8) using an osmotic stop flow technique. Usually, the decline has been interpreted to result from the development of the endodermis (2, 5, 7), the formation of an exodermis (13), or from changes of the hydraulic conductivity of cell membranes along the root (16). It should be noted that the corrected osmotic Lp_r may be an underestimate at distances of $z < 30$ mm from the root tip. In this area, both Lp_r (osmotic) as well as the axial conductance are low and water would have to overcome two resistances in series. For the tip, reliable data of Lp_r (osmotic) as well as of Lp_r (hydrostatic) are not available because axial and radial components could not be separated.

Axial resistances (R_x) have been measured in cutting experiments and by perfusing small root pieces. In addition, R_x

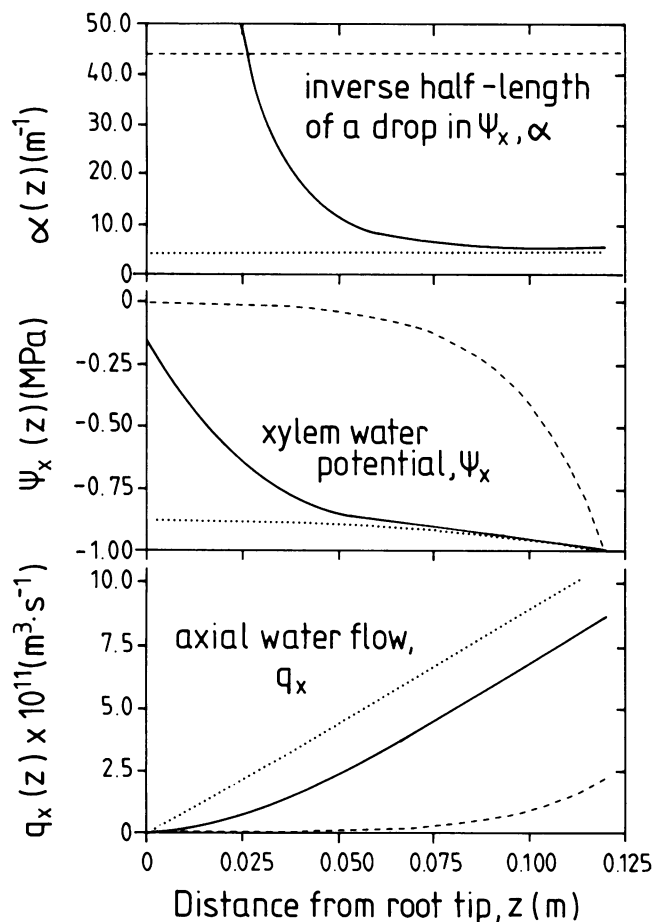


Figure 6. Calculated plots of Ψ_x and q_x as a function of root length at given values of α (= inverse of the half-length of a drop in Ψ_x) under stationary conditions. α is a measure of the ratio of R_x/R_R (Eq. 9). For the calculations, a root of length = 120 mm (mean diameter, $2 \cdot a = 1.3$ mm) was assumed. Profiles were obtained by numerical integration of Equations 7 and 10 assuming (a) measured (variable) values of R_x/R_R (solid line) and (b) estimated (constant) values of R_x/R_R (dotted and dashed lines). In case (a), R_R has been obtained from the hydrostatic experiments shown in Figure 3B. It can be seen from the figure that different characteristics of α strongly affect the gradients of xylem water potential along the root and, thus, the amount of water which can be taken up into the xylem.

has been calculated from xylem dimensions using Poiseuille's law. Calculated values of R_x were smaller than measured values by a factor of 2 to 5 (Table II). These differences may indicate that the assumption made of a viscous flow in an ideal cylindrical vessel did not hold (4). Another reason for the deviation may be attributed to the uncertainty to identify mature xylem vessels by the staining procedure used. Differences in R_x depending on the technique applied have been reported in the literature. Working with pea and wheat, Greacen *et al.* (6) found R_x being larger by a factor of 1.3 to 2.3 when measurements were compared with calculations. However, our data exclude a significant contribution of late metaxylem in axial water flow. It should be emphasized that assuming only one single conductive vessel of the late metaxylem would have decreased R_x by an order of magnitude.

The model of the root used here to describe effects of R_x

and R_R on Ψ_x and on the collection of water by the root (q_x) is analogous to that used for a leaky cable in electricity or in a nerve cell in electrophysiology (24). In fact, it has been already tried to employ electrophysiological techniques to measure the development of xylem in young roots of maize (1). However, this technique did not work because of cable effects, *i.e.* the radial flow of electric current (analog to water flow) was too large. This is different from the technique used here, where the development of the xylem could be followed. Since the radial hydraulic resistance per unit length was significantly larger than R_x (Table II), the rate limiting step in water uptake was the movement of water across the root cylinder.

The analysis of water uptake clearly shows that variable ratios of R_x/R_R strongly affect the profiles of Ψ_x and q_x (Fig. 6). A small ratio of R_x/R_R resulted in a monotonous increase of q_x at a distance between 30 and 120 mm from the apex, although the gradient for the driving force along the xylem ($d\Psi_x/dz$) was rather low (Eq. 6). On the other hand, in the tip region, water uptake was substantially restricted by the steep increase of R_x . According to Landsberg and Fowkes (9), regions of monotonous increase of q_x along the root define the effective root length in terms of water uptake. Therefore, the effective length of the segments used in this paper was close to the total length. However, it cannot be excluded that α could vary in older parts of the roots so that the picture of the segment could be different from that of a root system. For example, the calculated flow rates per unit area of effective surface area, J_{Vr} ($=q_T/A_r^{\text{eff}}$), in the present study were twice as high as in Miller's measurements of volume flows across root systems of maize assuming the same value of driving force (10). Since L_p was similar in both studies, the difference may indicate changes of α along the older, branched root system which could be due to suberization and subsequent increase of R_R . This shows that the influence of either radial or axial resistances on water flow cannot be discussed independently.

The calculation of L_p , using the pressure relaxation technique (as in this study) also requires the knowledge of R_x . In the simple two compartment model of the root, R_x should be significantly smaller than R_R , *i.e.* cable effects should be small. Except for the tip region, this assumption was fulfilled for maize, but also for roots of *Phaseolus* (20) to a fairly good approximation. For maize roots, the hydraulic conductivity (L_p) calculated from q_T , ($\Psi_x(c) - \Psi_s$), and effective root surface area resulted in an $L_p = 21 \cdot 10^{-8} \text{ m} \cdot \text{s}^{-1} \cdot \text{MPa}^{-1}$ which was 85% of the value found in relaxations. This indicated a good agreement between the measurement of transient and the calculation of stationary flows.

In order to reveal quantities and limiting steps for water uptake of complex root systems, additional information is required about the characteristics of $R_R(z)$ and $R_x(z)$ in older parts of the main root axis as well as in the laterals. Furthermore, a more rigorous modeling would require some knowledge of changes in the osmotic pressure in the root xylem due to the uptake and conduction of water and solutes in the root. These experiments and the subsequent modeling are presently performed using root segments as well as root systems.

ACKNOWLEDGMENTS

We thank Dr. C. A. Peterson, Department of Biology, University of Waterloo, Ontario, Canada, for reading and discussing the manuscript. We are also grateful to Sebastian Sommer for providing us with the program for the calculation of root profiles, and to Walter Melchior for performing some of the experiments.

LITERATURE CITED

1. Anderson WP, Higinbotham N (1976) Electrical resistances of corn root segments. *Plant Physiol* 57: 137-141
2. Brouwer R (1954) Water absorption by the roots of *Vicia faba* at various transpiration strength. III. Changes in water conductivity artificially obtained. *Proc K Ned Akad Wet C* 57: 68-80
3. Fiscus EL (1975) The interaction between osmotic and pressure induced water flow in plant roots. *Plant Physiol* 55: 917-922
4. Giordano R, Salleo A, Salleo S, Wanderlingh F (1978) Flow in xylem vessels and Poiseuille's law. *Can J Bot* 56: 333-338
5. Graham J, Clarkson DT, Sanderson J (1974) Water uptake by roots of marrow and barley plants. *Agr Res Council Letcombe Laboratory Report No. 1937*, pp 9-12
6. Greacen EL, Ponsana P, Barley KP (1976) Resistance to flow in the roots of cereals. In: OL Lange, L Kappen, E-D Schulze, eds, *Water and Plant Life. Problems and Modern Approaches*. Springer Verlag, Berlin, pp 86-100
7. Kramer PJ (1983) *Water relations of plants*. Academic Press, New York
8. Jones H, Leigh RA, Wyn Jones RG, Tomos AD (1988) The integration of whole-root and cellular hydraulic conductivities in cereal roots. *Planta* 174: 1-7
9. Landsberg JJ, Fowkes ND (1978) Water movement through plant roots. *Ann Bot* 42: 493-508
10. Miller DM (1985) Studies on root function of *Zea mays*. IV. Effects of applied pressure on hydraulic conductivity and volume flow through the excised root. *Plant Physiol* 77: 168-174
11. Newman EI (1976) Water movement through root systems. *Phil Trans R Soc Lond B* 273: 463-478
12. Passioura JB (1981) Water collection by roots. In LG Paleg, D Aspinall, eds, *The Physiology and Biochemistry of Drought Resistance in Plants*. Academic Press, New York, pp 39-53
13. Perumalla CJ, Peterson CA (1986) Deposition of Casparian bands and suberin lamellae in the exodermis and endodermis of young corn and onion roots. *Can J Bot* 64: 1873-1878
14. Peterson CA, Emanuel ME, Humphreys GB (1981) Pathway of movement of apoplastic fluorescent dye tracers through the endodermis at the site of secondary root formation in corn (*Zea mays*) and broad bean (*Vicia faba*). *Can J Bot* 59: 618-625
15. Pitman MG, Wellware D (1978) Inhibition of ion transport in excised barley roots by abscisic acid; relation to permeability of roots. *J Exp Bot* 29: 1125-1138
16. Radin JW, Matthews MA (1989) Water transport properties of cells in the root cortex of nitrogen- and phosphorus-deficient cotton seedlings. *Plant Physiol* 88: 264-268
17. Sanderson J (1983) Water uptake by different regions of the barley root. Pathways of radial flow in relation to development of the endodermis. *J Exp Bot* 34: 40-53
18. St Aubin G, Canny MJ, McCully ME (1986) Living vessel elements in the late metaxylem of sheathed maize roots. *Ann Bot* 58: 577-588
19. Steudle E (1989) An overview of water flows in plants and its coupling to other processes. In B Fleischer, S Fleischer, eds, *Biomembranes and Biological Transport. Volumes of Enzymology*, Vol 174 (in press)
20. Steudle E, Brinckmann E (1989) The osmometer model of the root: Water and solute relations of *Phaseolus coccineus*. *Bot Acta* 102: 85-95
21. Steudle E, Frensch J (1989) Osmotic responses of maize roots: water and solute relations. *Planta* 177: 281-295
22. Steudle E, Jeschke WD (1983) Water transport in barley roots. *Planta* 158: 237-248
23. Steudle E, Oren R, Schulze E-D (1987) Water transport in maize roots. Measurement of hydraulic conductivity, solute permeability, and of reflection coefficients of excised roots using the root pressure probe. *Plant Physiol* 84: 1220-1232
24. Taylor RE (1963) Cable Theory. In WL Nastuk, ed, *Physical techniques in biological research*, Vol IV, *Electrophysiological methods*, Part B. Academic Press, New York, pp 219-262